Fluorescence Intensity and Anisotropy Decays of the Intrinsic Tryptophan Emission of Hemoglobin Measured with a 10-GHz Fluorometer Using Front-Face Geometry on a Free Liquid Surface

E. Bucci,[1,2] Z. Gryczynski,[1] C. Fronticelli,[1] I. Gryczynski,[1] and J. R. Lakowicz[1]

We measured the intensity and anisotropy decays of the intrinsic tryptophan emission from hemoglobin solutions obtained using a 10-GHz frequency-domain fluorometer and a specially designed cuvette which allows front-face excitation on a free liquid surface. The cuvette eliminates reflections and stray emissions, which become significant for low-intensity fluorescence such as in hemoglobin. Three lifetimes are detectable in the subnanosecond range. The average lifetime of hemoglobin emission is ligand dependent. The measured values of average lifetimes are 91, 174, and 184 ps for deoxy-, oxy-, and carboxyhemoglobin, respectively. Fluorescence anisotropy decays of oxy-, deoxy-, and carbonmonoxyhemoglobin can be fitted with up to three correlation times. When three components are used, the floating initial anisotropy r_0 is, in each case, higher than the steady-state anisotropy of tryptophan in vitrified solution. For deoxy hemoglobin it is close to 0.4. The data are consistent with an initial loss of anisotropy from 0.4 to about 0.3 occurring in the first 2 ps.

INTRODUCTION

The intrinsic tryptophan emission from protein has been widely used to investigate protein conformation and dynamics. However, in spite of considerable interest in hemoglobin (Hb), fluorescence studies of its tertiary and quaternary conformational changes have been hindered by the weak tryptophan emission, which is known to be strongly quenched by energy transfer to the heme [1,2]. Ligand binding to Hb can induce changes in tryptophan–

heme distances and orientations, which can affect energy transfer, possibly revealed by changes in lifetimes. For this reason, time-resolved fluorescence of hemoglobin is of great interest and has been investigated by several groups for nearly a decade [3–7].

The strong quenching of tryptophan by the heme poses the problem of detecting and interpreting emission signals with a very low intensity. As shown by Bucci *et al.* [7], the emission of hemoglobin has an intensity much lower than the scattering of incident light by the solution and, in square geometry optics, is dominated by Raman scattering. Although these difficulties can be eliminated by the use of front-face techniques and cutoff filters [7], additional precautions are necessary. The samples must be extremely pure in order to avoid the presence of im-

[1] Department of Biological Chemistry and Center for Fluorescence Spectroscopy, University of Maryland at Baltimore, 660 West Redwood Street, Baltimore, Maryland 21201.
[2] To whom correspondence should be addressed.

purities whose emission is not quenched by the heme. Also, special attention must be rendered to reflections and other stray light in the emissions, which may be as intense as the fluorescence itself. Using front-face technology, one should also consider surface denaturation of hemoglobin at the contact between the solution and the cuvette window. In order to avoid these problems, we have used a specially designed cuvette which minimizes reflections and allows front-face geometry where the incident light falls on a free liquid surface.

With regard to anisotropy decay, Bucci and co-workers [8-15] obtained data with hemoglobin systems labeled at the β93 cysteines with probes whose residual lifetime after coupling was about 1 ns. Those data indicated that hemoglobin is not a solid rotator and is endowed with internal motions which prevent observation of the rotational behavior of the entire tetramer. Those data also showed that in deoxyhemoglobin, the internal mobility of the molecule is inhibited, indicating a more compact structure than in liganded hemoglobin. Those data were obtained with probes whose lifetimes were about 1 ns; in contrast, the lifetime of tryptophan residues in hemoglobin is very short and the anisotropy decays should contain rich information about fast processes.

MATERIALS AND METHODS

Human hemoglobin was prepared and purified by HPLC techniques as described elsewhere [6].

Fluorescence lifetimes and anisotropies were measured using a 10-GHz fluorometer equipped with a Hamamtsu 6-μm microchannel plate detector (MCP-PMT), as described previously [16].

The design and characteristics of the cuvette used for front-face geometry on a free liquid surface are described in another article [Z. Gryczynski et al., in preparation]. It is, essentially, a cup in which the solution under examination forms a free liquid surface in contact only with the gas in the chamber. As shown schematically in Fig. 1, the cover of the cuvette is designed to shield the excitation from the emission beam and to deflect and/or absorb stray reflections from the liquid surface. Additional diaphragms can be used to allow only the light emitted in a direction perpendicular to the liquid surface to reach the MCP-PMT. The absence of reflections and of unwanted stray emissions was proven by the inability of the MCP-PMT to detect any signal when the cuvette was filled either with water or with a ludox (scatterer) suspension.

For anisotropy measurements, the incident light at

300 nm was polarized in a plane parallel to the surface of the liquid, with a vector perpendicular to the plane described by the excitation and emission beams, i.e., to the plane of the paper in Fig. 1. In the emission, we used an interference filter centered at 335 nm with a bandpass of 30 nm and a Corning 0-54 filter with a cutoff at 340 nm. For reference, we used the scattering of the hemoglobin solutions by substituting the filters, in the emission path, with an interference filter centered at 298 nm with a bandpass of 10 nm and a neutral density filter, which lowered the intensity of the signal to levels compatible with the fluorescence intensity. The phase delay produced by the two (sample and reference) sets of filters was calibrated at the proper wavelength with an accuracy better than 1 ps. We used hemoglobin solutions with optical densities near 20 in a 1-cm path, at the wavelength of excitation light.

The accuracy of the cuvette in providing anisotropy data was determined by two steady-state measurements. First, we measured the fluorescence anisotropy at 580 nm of pyrene in hexane at concentrations sufficient to produce excimer. As expected, the anisotropy value was 0.00. Second, we measured the polarization spectrum of tryptophan (5×10^{-4} M) in glycerol at $-5°C$. In the free surface cuvette, the addition of hemin increased the optical density of the sample so as to prevent penetration of the exciting light into the solution, with consequent secondary reflections on the walls of the cup. The concentrations of tryptophan and hemin were too low for producing detectable energy transfer phenomena. This spectrum was compared to that obtained in classic square geometry with an identical solution of tryptophan. Figure 2 shows that the two spectra were superimposable and that maximum anisotropy was reached at an excitation wavelength of 300 nm.

TREATMENT OF THE DATA

Intensity decays were measured using magic-angle polarization conditions which eliminate the effects of rotational motions on the decay [17]. The frequency-dependent phase (ϕ_ω) and modulation (m_ω) values were fitted to a multiexponential decay law,

$$I(t) = \sum_i \alpha_i e^{-t/\tau_i} \qquad (1)$$

as described previously [18]. In this expression α_i and τ_i are the amplitude and decay time, respectively, of the
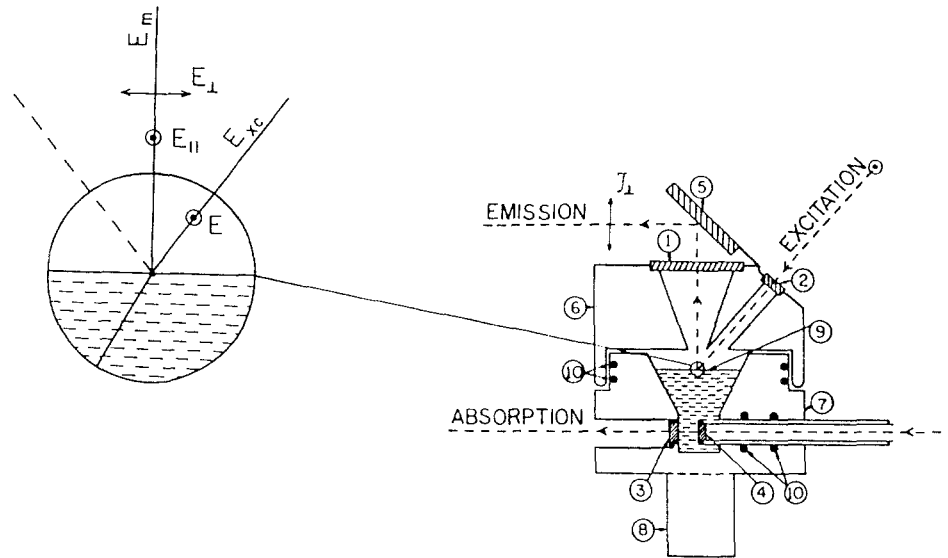
Fig. 1. Side view of the free-surface cuvette. (1–3) Fixed quartz windows; (4) sliding quartz window; (5) metallic mirror; (6) body of the cover; (7) body of the cuvette; (8) supporting stem; (9) liquid surface of sample; (10) "O" rings. Polarizers and filters are positioned as usual in the excitation and emission paths. Surface metallic mirrors were chosen which did not affect the polarization of the incident light.
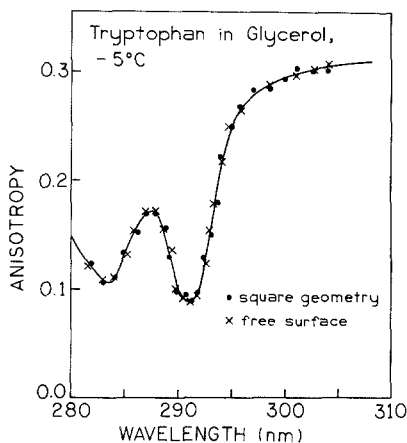

Fig. 2. Steady-state excitation polarization spectrum of tryptophan in glycerol solutions at −5°C, using square geometry (●), compared to that of tryptophan in the free-surface cuvette (X).

*i*th component. The fractional intensity (f_i) of each component of the emission was obtained from

$$f_i = \alpha_i \tau_i / \sum_j \alpha_j \tau_j \qquad (2)$$

For anisotropy decay measurements the sample was excited with light polarized as described above, which was intensity modulated. We measured the phase angle

difference (Δ_ω) between the perpendicular and the parallel components of the modulated emission,

$$\Delta\omega = \phi_\perp - \phi_\| \qquad (3)$$

and the ratio of the amplitudes of the modulated emission (Λ_ω),

$$\Lambda_\omega = m_\| / m_\perp \qquad (4)$$

The subscript ω refers to the modulation frequency (rad/s). The modulated amplitude data are better understood by using the modulated anisotropy,

$$r_\omega = \frac{\Lambda_\omega - 1}{\Lambda_\omega + 2} \qquad (5)$$

At low frequencies r_ω becomes equivalent to the steady-state anisotropy. At high frequencies it becomes equal to the fundamental anisotropy with no rotational diffusion (r_0).

The frequency-domain data (Δ_ω and Λ_ω) were fitted to a multiexponential anisotropy [$r(t)$] decay model,

$$r(t) = r_0 \sum_i g_i\, e^{-t/\theta_i} \qquad (6)$$

where θ_i are the correlation times, g_i are the associated amplitudes, and r_0 is the limiting anisotropy at zero time. In the simulations the value of r_0 was either left floating or fixed at 0.4.

The quality of fit was assessed by reduced chi-square

(χ_R^2), which is the sum of the squared deviations weighted by the variance of the measurements, normalized to the degrees of freedom of the system (ν),

$$\chi_R^2 = \frac{1}{\nu} \sum_{\omega} \left(\frac{\Delta_\omega - \Delta_{\omega c}}{\delta\Delta} \right)^2$$

$$+ \frac{1}{\nu} \sum_{w} \left(\frac{\Lambda_\omega - \Lambda_{\omega c}}{\delta\Lambda} \right)^2 \quad (7)$$

in the equation the subscripts ω and ωc refer to experimental and calculated values, and $\delta\Delta$ and $\delta\Lambda$ are the errors for phase and modulation measurements, respectively. A similar procedure was used to analyze the intensity decay $I(t)$ in terms of individual lifetimes.

RESULTS

Phase and modulation data for deoxy-, oxy-, and carbonmonoxyhemoglobin are presented in Figs. 3 and 4. Three different preparations were tested with very similar results. We present here data obtained from a single experiment. Table I shows the lifetimes recovered using one-, two-, or three-component fits. In parentheses are the 67% confidence limits. In each case, the best value of chi-square was obtained with three decay times
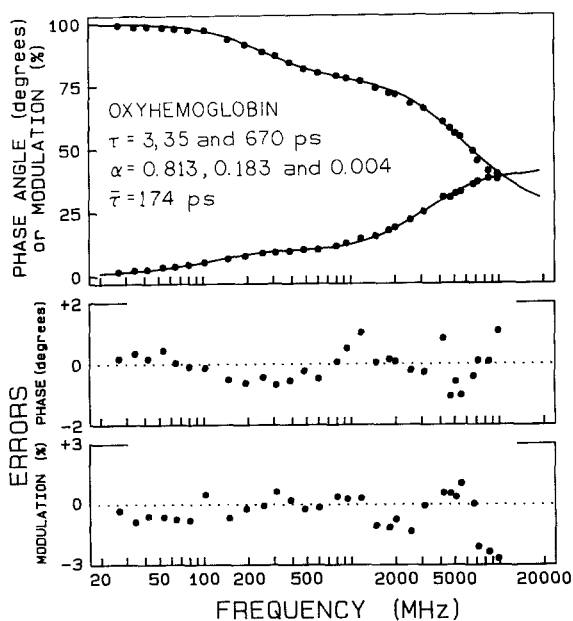

Fig. 4. Phase and modulation intensity decay data for deoxy (•)- and carbonmonoxy (▲)- hemoglobin. The solid lines show the best three-lifetime fit to the data. The upper curves are for modulation data.

and all decay times were in the subnanosecond range; no lifetimes were found in the nanosecond range. This was probably due to the purity of the samples, the lack of stray light, reflections, and the absence of surface denaturation of the protein in contact with the quartz window, as in classic cuvettes.

The frequency-domain anisotropy data for deoxy-, oxy-, and carbonmonoxyhemoglobin are presented in Figs. 5–7. The solid lines are three-exponential fits to the data. The recovered parameters of the anisotropy decays are summarized in Table II, together with their 67% confidence limits (values in parentheses). The chi-square values for the two- and three-component fits are not very different. The data presented in Table II were obtained leaving the value of r_0 floating in the computer analyses. Its value was higher than 0.32 in all cases and was 0.39 for deoxyhemoglobin. We have measured $r_0 = 0.30$ for free tryptophan in glycerol at $-5°C$. The normalized chi-square surfaces presented in Figs. 8 and 9 suggest a good definition of the estimated parameters. When the value of r_0 was fixed at 0.4, similar data were obtained, with a reduction of the span and the confidence limits, and a narrowing of the chi-square surfaces (shown in Fig. 8), as expected from the reduced degrees of freedom of the system.

The decay in time of the three-component anisotropy of deoxyhemoglobin was computed from the frequency-domain data and is presented in Fig. 10, so that readers can easily perceive the shape of the anisotropy decay curve.

Fig. 3. Phase and modulation intensity decay data for oxyhemoglobin. The solid lines show the best three-lifetime fit to the data. The upper curve is for modulation data. The lower panels present the deviations in phase and modulation between the calculated and the measured values.
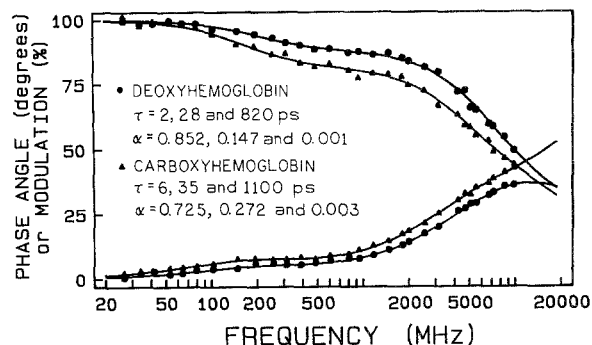
DISCUSSION

The combination of 10-GHz fluorometry with a specially designed cuvette probably represents a break-

Table I. Multiexponential Intensity Decay of Hemoglobin

Compound	n^a	$\bar{\tau}_i$ $(ps)^b$	τ_i (ps)		α_i	f_i	χ_R^2
Deoxyhemoglobin	1		18		1	1	486.8
	2		15		0.991	0.80	
			41		0.009	0.20	93.1
	3		2	$(1.2–2.9)^c$	0.852	0.25	
			28	(27.3–28.6)	0.147	0.66	
		91	820	(766–873)	0.001	0.09	5.1
Oxyhemoglobin	1		33		1	1	1134.9
	2		17		0.978	0.67	
			36		0.022	0.33	119.6
	3		3	(2.2–4.0)	0.813	0.23	
			35	(33.7–36.2)	0.183	0.54	
		174	670	(665–714)	0.004	0.23	4.7
Carboxyhemoglobin	1		23		1	1	851.9
	2		19		0.990	0.74	
			64		0.010	0.26	103.5
	3		6	(4.6–7.3)	0.725	0.31	
			35	(33.7–37.2)	0.272	0.54	
		184	1100	(1012–1188)	0.003	0.15	5.4

^{a} Number of exponential components.
^{b} $\bar{\tau} = \Sigma_i f_i \tau_i$.
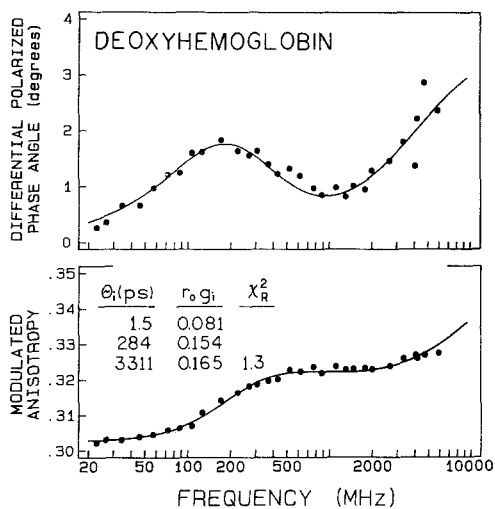^{c} From 67% confidence limits.

Fig. 5. Differential phase and modulated anisotropy data for deoxy-hemoglobin. The solid lines show the best three-correlation time fit to the data.
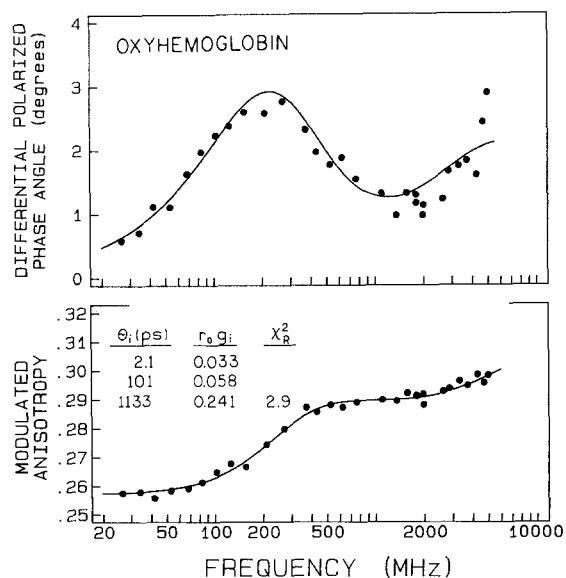

Fig. 6. Differential phase and modulated anisotropy data for oxyhemo-globin. The solid lines show the best three-correlation time fit to the data.

through in the investigation of hemoglobin fluorescence. The absence of reflections or other signals from the cu-vette filled with water or ludox suspension suggests that even the shortest lifetimes, single-digit picoseconds, originated from hemoglobin. It may be argued that the single-digit picosecond lifetimes were dependent on the

last two or three determinations at high frequency, where instrumental factors may play a bigger role. We are mea-suring the distance and angular relationships between tryptophans and hemes in hemoglobin, and in a manu-
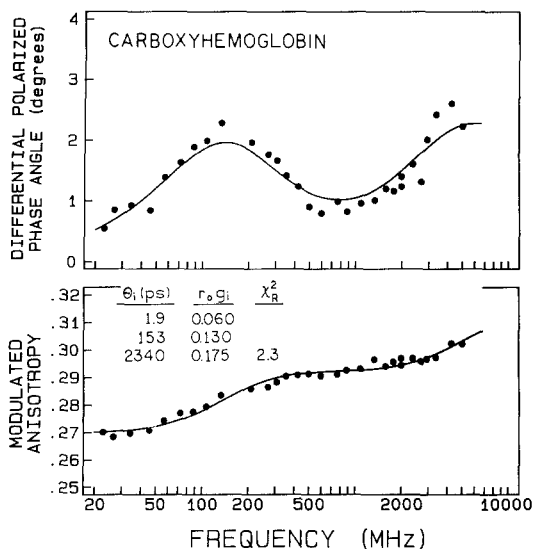
Fig. 7. Differential phase and modulated anisotropy data for carboxy-hemoglobin. The solid lines show the best three-correlation time fit to the data.

Table II. Multiexponential Anisotropy Decay of Hemoglobin

Compound	n^a	θ_i (ps)		$r_0 g_i$	χ_R^2
Deoxy-Hb	1	663		0.331	7.1
	2	33	$23-100^b$	0.061	
		1182	(1086–1836)	0.286	1.9
	3	1.8	(1.4–2.5)	0.073	
		283	(252–315)	0.152	
		3238	(2748–4165)	0.167	1.3
Oxy-Hb	1	657		0.029	8.1
	2	57	(34–87)	0.056	
		1052	(929–1216)	0.254	3.0
	3	2.1	(1.2–3.2)	0.033	
		101	(94–110)	0.058	
		1133	(1059–1217)	0.241	2.8
Carboxyl-Hb	1	545		0.306	9.7
	2	102	(79–131)	0.122	
		1975	(1500–2579)	0.194	2.4
	3	1.9	(1.2–2.6)	0.060	
		153	(145–160)	0.130	
		2340	(1985–2837)	0.175	2.2

^{a} Number of exponential components.
^{b} From 67% confidence intervals.

Fig. 8. χ_R^2 surfaces for the correlation times of deoxyhemoglobin.

Fig. 9. χ_R^2 surfaces for the fractional anisotropy decay correspondent to the correlation times of deoxyhemoglobin.

script submitted for publication, we are presenting data demonstrating that single-digit picosecond lifetimes are justified by the crystal coordinates of hemoglobin.

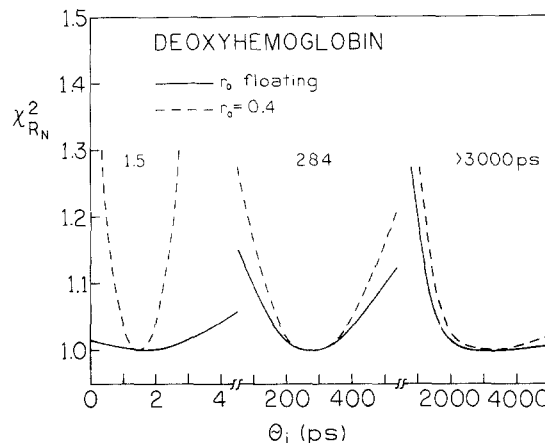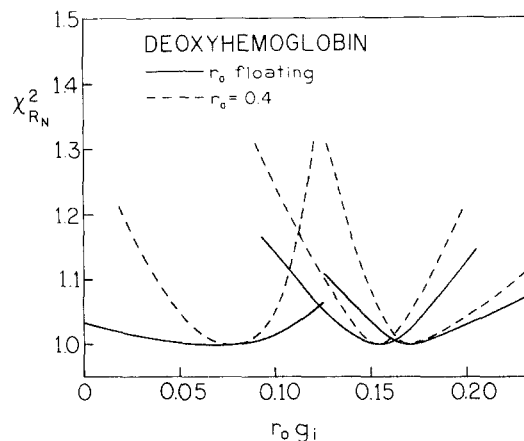The ligand dependence of the lifetimes deserves attention. Whereas average lifetimes of oxy- and carbon-monoxyhemoglobin are similar (174 and 189 ps, respectively), the average lifetime of deoxyhemoglobin is almost twice as short (91 ps). Because the overlap integrals (tryptophan fluorescence and heme absorption) for oxy- and deoxyhemoglobin are very similar (Z. Gryczynski, in preparation), the most probable explanation of the two-fold reduction of the average lifetimes is the conformational changes induced by ligand binding in hemoglobin. The heme acquires a different tilting with respect to the proximal histidine upon ligand binding [9]. This may modify its relative angular position with regard to the tryptophans, thereby altering the energy transfer in a ligand linked fashion. We are currently investigating the effect of the heme tilting, based on the crystal coordinates of liganded and unliganded hemoglobin.

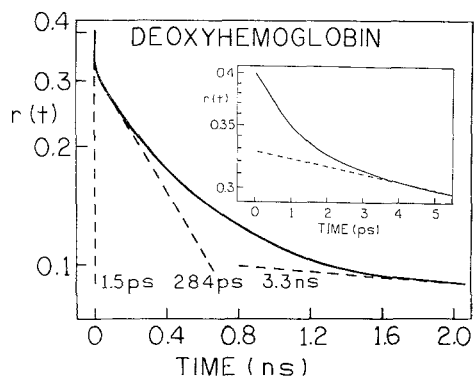The anisotropy decays were fitted to three expo-

Fig. 10. Time-domain representation of the three-component anisotropy decay of deoxyhemoglobin. The inset shows an enlarged view of the first 5 ps of the decay.

nentials where r_0 was a floating parameter. In each case, the fitted r_0 value was larger than the steady-state value obtained for tryptophan in vitrified solutions (0.31–0.32 in our laboratory). For deoxyhemoblogin, where the average lifetime is only 91 ps, the fitted r_o was almost 0.4 (0.39). For all hemoglobin derivatives, two- or three-component analyses gave very similar statistics, the three-component simulations indicated the presence of a fast correlation time, about 2 ps, during which 10 to 15% of the initial anisotropy was lost.

These data confirm and better define the finding of Bucci et al. [6] that the value of the initial anisotropy (at time zero) of tryptophan in hemoglobin is higher than that measured in the steady state for frozen tryptophan. Also, in those experiments the observation was extended only up to 2 GHz, and only two correlation times could be detected. Notably, the shortest of the correlation times of those early measurements (near 60 ps) are very consistent with the shortest of the two-component analyses shown in Table II.

There are several possible explanations for the rapid initial anisotropy loss shown by the three-component analyses; fast vibrational relaxation in excited-state and torsional motions of indole ring. The most probable explanation seems to be involvement of the second excited-state ^1L_b into fluorescence kinetics. The internal conversion rate between ^1L_a and ^1L_b states in tryptophan has been estimated recently by Fleming and co-workers to be near 1.6 ps from upconversion measurements [20,21]. They also reported a value very close to 0.4 for the initial anisotropy of tryptophan fluorescence. Those data are consistent with our findings.

The longer correlation times, in the picosecond range, probably show the local mobility of tryptophan and the

correlation times in the nanosecond range suggest the presence of internal flexibility of the hemoglobin molecule. It should be stressed that, under the conditions of the experiments, the expected correlation times are near 30 ns for the hemoglobin tetramer and near 8 ns for a single subunit, respectively [15]. This is consistent with the early findings of Bucci and colleagues [8–10], who showed the presence in liganded hemoglobin of structural domains with correlation times near 5 ns. Also, those early data showed that the internal motions of hemoglobin are somewhat inhibited in deoxyhemoglobin. In a consistent fashion, the data here presented show that the local mobility of the tryptophans is inhibited upon removal of ligands.

ACKNOWLEDGMENTS

REFERENCES

1. G. Weber and F. J. W. Teale (1959) Disc. Faraday Soc. 27, 134–141.
2. B. Alpert, D. M. Jameson, and M. Zuker (1984) Photochem. Photobiol. 31, 1–34.
3. A. G. Szabo, D. Krajcarski, and M. Zucker (1984) Chem. Phys. Lett. 108, 145–152.
4. J. Albani, B. Alpert, D. Krajcarski, and A. G. Szabo (1985) FEBS Lett. 182, 302–306.
5. R. M. Hochstrasser and D. K. Negus (1984) Proc. Natl. Acad. Sci. USA 81, 4399–4405.
6. E. Bucci, H. Malak, C. Fronticelli, I. Gryczynski, and J. R. Lakowicz (1988) J. Biol. Chem. 263, 6972–6977.
7. E. Bucci, H. Malak, C. Fronticelli, I. Gryczynski, G. Laczko, and J. R. Lakowicz (1988) Biophys. Chem. 32, 187–198.
8. E. Bucci, C. Fronticelli, J. Perlman, and R. F. Steiner (1979) Biopolymers 18, 1261.
9. J. Oton, E. Bucci, R. F. Steiner, C. Fronticelli, D. Franchi, J. X. Montemarano, and A. Martinez (1981) J. Biol. Chem. 256, 7248–7256.
10. M. Sassaroli, E. Bucci, and R. F. Steiner (1982) J. Biol. Chem. 257, 10136–10140.
11. J. Kowalczyk and E. Bucci (1983) Biochemistry 22, 4805–4809.
12. M. Sassaroli, E. Bucci, J. Liesegang, C. Fronticelli, and R. F. Steiner (1984) Biochemistry 23, 2487–2491.
13. J. Oton, D. Franchi, R. F. Steiner, C. Fronticelli, A. Martinez, and E. Bucci (1984) Arch. Biochem. Biophys. 228, 519–524.
14. M. Sassaroli, J. Kowalczyk, and E. Bucci (1986) Arch. Biochem. Biophys. 25, 624–628.
15. E. Bucci and R. F. Steiner (1988) Biophys. Chem. 30, 299–324.
16. G. Laczko, I. Gryczynski, G. Gryczynski, W. Wiczk, H. Malak, and J. R. Lakowicz (1990) Rev. Sci. Instrum. 61, 2331–2337.

17. R. D. Spencer and G. Weber (1970) *J. Chem. Phys.* **52,** 1654–1659.

18. J. R. Lakowicz, E. Gratton, G. Laczko, H. Cherek, and M. Limkeman (1984) *Biophys. J.* **46,** 463–477.

19. J. Baldwin and C. Chotia (1979) *J. Mol. Biol.* **129,** 175–219.

20. A. Cross, D. H. Waldeck, and G. R. Flemming (1990) *J. Chem. Phys.* **78,** 6455–6467.

21. A. J. Ruggiero, D. C. Todd, and G. R. Flemming (1990) *J. Am. Chem. Soc.* **112,** 1003–1014.